

Protein Kinase C θ Regulates Stability of the Peripheral Adhesion Ring Junction and Contributes to the Sensitivity of Target Cell Lysis by CTL¹

Allison M. Beal,* Nadia Anikeeva,* Rajat Varma,^{2†} Thomas O. Cameron,[†] Philip J. Norris,[‡] Michael L. Dustin,[†] and Yuri Sykulev^{3*}

Destruction of virus-infected cells by CTL is an extremely sensitive and efficient process. Our previous data suggest that LFA-1-ICAM-1 interactions in the peripheral supramolecular activation cluster (pSMAC) of the immunological synapse mediate formation of a tight adhesion junction that might contribute to the sensitivity of target cell lysis by CTL. Herein, we compared more (CD8⁺) and less (CD4⁺) effective CTL to understand the molecular events that promote efficient target cell lysis. We found that abrogation of the pSMAC formation significantly impaired the ability of CD8⁺ but not CD4⁺ CTL to lyse target cells despite having no effect of the amount of released granules by both CD8⁺ and CD4⁺ CTL. Consistent with this, CD4⁺ CTL break their synapses more often than do CD8⁺ CTL, which leads to the escape of the cytolytic molecules from the interface. CD4⁺ CTL treatment with a protein kinase C θ inhibitor increases synapse stability and sensitivity of specific target cell lysis. Thus, formation of a stable pSMAC, which is partially controlled by protein kinase C θ , functions to confine the released lytic molecules at the synaptic interface and to enhance the effectiveness of target cell lysis. *The Journal of Immunology*, 2008, 181: 4815–4824.

Cytotoxic T lymphocyte detection and lysis of target cells is facilitated by adhesion molecules such as LFA-1 and CD2 that promote Ag-nonspecific interactions (1, 2). Ag-nonspecific adhesion precedes the interaction of TCR with cognate peptide-MHC (pMHC)⁴ (3). Recognition of agonist pMHC complexes on the target cell surface induces CTL arrest of migration and molecular segregation of TCR and adhesion molecules into a bull's-eye pattern at the T cell-target cell interface, which has been designated the immunological synapse (IS) (4). The zones of the bull's-eye pattern are defined from outside ring to center as the distal, peripheral, and central supramolecular activation clusters (dSMAC, pSMAC, and cSMAC, respectively) (5). The dSMAC is a peripheral lamellipodium containing CD45 and dynamic actin; the pSMAC is an adhesion ring; and the cSMAC is a site of TCR, pMHC, and lytic granule concentration (4–9). When the symmetry of the pSMAC is broken, the stable IS may convert into a horseshoe-like adhesive junction or kinapse (10, 11). While the role of

a stable pSMAC in the sensitivity of target cell lysis by CD8⁺ CTL has been unveiled (8), how the horseshoe-like adhesive junction influences cytolytic activity is not known.

Although it appears that the cSMAC plays a critical role for the delivery of cytolytic granules (12), the mechanism by which the pSMAC contributes to cytolytic activity is not entirely clear. We have observed that granule release by CD8⁺ CTL is confined to the cSMAC (A. M. Beal, N. Anikeeva, R. Varma, T. O. Cameron, P. J. Norris, M. L. Dustin, and Y. Sykulev, manuscript in preparation) and that complete disruption of ICAM-1-LFA-1 interactions in the pSMAC strongly reduces target cell lysis without impairing granule release (8). Furthermore, we have demonstrated that CD8⁺ CTL form a ring junction similar to the pSMAC in the absence of Ag and proposed that the pSMAC functions as a gasket for efficient delivery of lytic molecules to target cells (13).

While cytolytic activity is usually exercised by CD8⁺ CTL, which play a critical role in containing the spread of viruses, some viral infections, such as HIV (14–16) and EBV (17, 18), are often characterized by the presence of CD4⁺ CTL. Numerous experimental observations suggest that CD4⁺ CTL are less potent lytic effectors than CD8⁺ CTL (19), and their role in chronic viral infection is not entirely clear. Nonetheless, these cells provide an opportunity to probe characteristics that define sensitivity of target cell lysis by comparison to CD8⁺ CTL.

Herein we demonstrate that the pSMAC indeed functions to confine the released lytic molecules at the synaptic interface and that protein kinase C θ (PKC θ) contributes to the disruption of the pSMAC, which reduces the effectiveness of CD4⁺ CTL by favoring formation of a crescent adhesive junction that lacks the pSMAC gasket.

Materials and Methods

Cells

The human CD4⁺ CTL clones AC-25 and 161J, which recognize PEVIMPFALSEGATP (PP16) and PEVIMPFALSEG (PG13) peptides, respectively, from the HIV Gag protein, were derived from HIV-infected subjects as described (14, 20). The human CD8⁺ CTL clone (CER43) that

*Department of Microbiology and Immunology and Kimmel Cancer Institute, Thomas Jefferson University, Philadelphia, PA 19107; [†]Skirball Institute of Biomolecular Medicine, New York University School of Medicine, New York, NY 10016; and [‡]Blood Systems Research Institute and the Departments of Laboratory Medicine and Medicine, University of California, San Francisco, CA 94118

Received for publication January 23, 2008. Accepted for publication August 1, 2008.

The costs of publication of this article were defrayed in part by the payment of page charges. This article must therefore be hereby marked *advertisement* in accordance with 18 U.S.C. Section 1734 solely to indicate this fact.

¹ This work was supported by NIH grants to Y.S. (AI3254), P.J.N. (AI067854), and M.L.D. (AI44931; AI3254). A.M.B. was supported in part by NRSA training grant T32-CA 0983.

² Current address: National Institute of Allergy and Infectious Diseases/Laboratory of Cellular and Molecular Immunology, National Institutes of Health, Building 4, Room 431, 4 Center Drive, Bethesda, MD 20892.

³ Address correspondence and reprint requests to Dr. Yuri Sykulev, Department of Microbiology and Immunology, Kimmel Cancer Center, BLSB 706, Thomas Jefferson University, Philadelphia, PA 19107. E-mail address: sykulev@lac.jci.tju.edu

⁴ Abbreviations used in this paper: pMHC, peptide-MHC; cSMAC, central supramolecular activation cluster; dSMAC, distal supramolecular activation cluster; IS, immunological synapse; PKC θ , protein kinase C θ ; pSMAC, peripheral supramolecular activation cluster; RU, relative units; TIRF, total internal reflection fluorescence.

recognizes GILGFVFTL (GL9) peptide from the matrix protein of influenza virus (21, 22) was a gift from Antonio Lanzavecchia (Institute of Immunology, Bellinzona, Italy). The human HIV-specific CD8⁺ CTL clone 68A62 that recognizes the reverse transcriptase-derived peptide ILKEPVHGV (IV9) was a gift from Bruce D. Walker (Partners AIDS Research Center, Massachusetts General Hospital, Harvard Medical School, Boston, MA). The T2 (HLA-A2⁺) lymphoblast cell line transfected with HLA-DR1 and HLA-DR4 (designated T2-DR1 and T2-DR4, respectively) was a gift from Lisa Denzin (Memorial Sloan Kettering Cancer Center, New York, NY). C1R (CRL-1993), a human B lymphoblast cell line that does not express any HLA A or B gene products (23), was purchased from the American Type Culture Collection (ATCC).

Proteins and peptides

His₆-tagged HLA-A2 molecules were expressed, purified, and loaded with peptide of interest as previously described (24, 25). Truncated HLA-DR1 α (DRA*0101) and β (DRB1*0101) genes cloned in the pRmHa-3 vector were kindly provided by Larry Stern (University of Massachusetts Medical School, Worcester, MA), and a His₆ tag was introduced at the C terminus of the α -chain by cloning in the pMT/V5-HisA vector (Invitrogen). Soluble empty His₆-tagged HLA-DR1 molecules were expressed in insect cells and purified as previously described with some modifications (26). Protein expression was induced by CuSO₄, and the culture supernatant was concentrated and dialyzed against PBS (pH 8.0). Soluble DR1 molecules were isolated by immunoaffinity chromatography using HLA-DR-specific mAbs (L243) coupled to cyanogen bromide-activated Sepharose (GE Healthcare) and then loaded with peptide for 24–30 h at 37°C in Dulbecco's PBS (Cellgro) with 1 mM EDTA, 1 mM PMSF, 0.1 mM iodoacetamide, and 3 mM NaN₃. Peptide-loaded DR1 molecules were purified via Ni-NTA affinity chromatography (Qiagen) to isolate molecules with an intact His₆ tag followed by gel filtration on a Superdex 200HR to remove aggregated DR1 and residual contaminating proteins. For some experiments, purified DR1-peptide and HLA-A2-peptide complexes were labeled with Alexa Fluor 488 as per the manufacturer's instructions (Molecular Probes/Invitrogen).

PP16 from HIV p24 Gag (14) was synthesized by BioSynthesis, and PG13 from HIV p24 Gag was synthesized by Genemed Synthesis. Control peptides SDWRFLRGYHQYA from HLA-A2 and RVEYHFLSPYVSP KESP from transferrin receptor that have been identified as predominant self peptides bound to HLA-DRB1*0101 (27) were kindly provided by Larry Stern (University of Massachusetts Medical School, Worcester, MA). GL9 peptide from the influenza matrix protein was synthesized by Research Genetics, and IV9 peptide from HIV reverse transcriptase (28) was a gift from Herman N. Eisen (Center for Cancer Research and Department of Biology, Massachusetts Institute of Technology, Cambridge, MA).

Antibodies

Anti-CD107a (LAMP-1) Ab H4A3 was purchased from BD Pharmingen. We also purified anti-CD107a mAbs produced by hybridoma H4A3 (kindly provided by Dr. J. Thomas August, Department of Pharmacology and Molecular Sciences, Johns Hopkins Medical School, Baltimore, MD). Monovalent Fab fragments of anti-CD107a were produced by papain digestion and then purified by anion-exchange chromatography on Mono Q column (GE Healthcare). Purified Fab fragments were then labeled with Alexa Fluor 568 (Molecular Probes/Invitrogen). Anti-CD3 Ab were produced and purified from hybridoma HB10166 purchased from ATCC, and Fab fragments were prepared as above. Hybridomas L243 producing anti-HLA-DR and TS1/22 producing anti-LFA-1 Abs were purchased from ATCC, and the Abs were purified from culture supernatant by affinity chromatography on protein A-Sepharose. FITC-conjugated anti-perforin (clone 27-35) and PE-conjugated anti-granzyme A (clone MOPC-21) Abs were from BD Pharmingen. PE-conjugated anti-granzyme B (clone GB12) Ab was from Caltag Laboratories.

Cytolytic assay

T2-DR1 or T2-DR4 target cells (5×10^3) were washed, ⁵¹Cr-labeled, and then sensitized for 1 h with various amounts of peptide in 150 μ l R10 (RPMI 1640 containing 10% FCS). Effector CTL were then added in 50 μ l of R10 with a final assay volume of 200 μ l. In some experiments, anti-LFA-1 Abs TS1/22 were added to the wells at the final concentration of 10 μ g/ml. The assays were performed in 96-well round-bottom plates at an E:T ratio of 5:1. The plates were incubated for 4 h in a CO₂ incubator at 37°C, and ⁵¹Cr release was measured in 100 μ l of supernatant from each well. Percentage specific lysis was determined as previously described (29).

For some experiments anti-CD3 Fab were used to induce cytolytic activity. In these experiments 1×10^4 target cells (C1R) were ⁵¹Cr-labeled

and placed to wells of a 96-well round-bottom plate. Anti-CD3 Fab was added at various concentrations before the addition of effectors (CTL) at an E:T ratio of 5:1. The plates were then incubated and assayed for ⁵¹Cr release as above.

Granule release assay

T2-DR1 or T2-DR4 target cells (1×10^5) were washed and then sensitized for 1 h with various concentrations of peptide. CTL were then added with a final volume of 200 μ l and an E:T ratio of 5:1. Some assays were performed in the presence of anti-LFA-1 Abs TS1/22 at the final concentration of 10 μ g/ml. The assays were performed in 96-well round-bottom plates and incubated for 4 h at 37°C in CO₂ incubators. After the incubation, 100 μ l of supernatants was collected and the serine esterase activity, an essential component of released granules (30), was measured using the BLT (*N*-benzyloxycarboxyl-L-lysine thiobenzyl ester) substrate in the presence of DTNB (5',5'-dithio-bis(2-nitrobenzoic acid)) by reading the OD at 405 nm as described previously (8, 31).

In some experiments CTL were added to 5×10^4 target cells (C1R) at an E:T ratio of 5:1 in the presence of anti-CD3 Fab at various concentrations to trigger granule release. The assays were performed in 96-well round-bottom plates for 4 h at 37°C, and serine esterase release was measured as described above.

Granule isolation

Granules were isolated using Percoll density gradient fractionation as previously described (32, 33). Granule-containing fractions were identified by testing for serine esterase activity. The positive fractions were subsequently pooled and used in serine esterase and chromium-release assays.

Inhibition of PKC θ

The PKC θ inhibitor (compound 20) was provided by Boehringer Ingelheim (34). For cytolytic and granule release assays in which PKC θ was inhibited, T cells were pretreated with the inhibitor or DMSO control for 5 min at 37°C. T cells plus inhibitor were added to peptide-sensitized target cells and incubated for 4 h as indicated above. For treatment of CTL for use in lipid bilayer experiments, inhibitor was added before adding the T cells to the flow cells containing the lipid bilayers. The final concentration of PKC θ inhibitor used in the assays was 1 μ M.

Planar lipid bilayers and microscopy

Planar lipid bilayers were prepared in parallel-plate flow cells as described previously (4, 8, 13). Liposomes containing Cy5-ICAM-1-GPI were placed on a clean glass to form the planar bilayer with a final density of ICAM-1 around 300 molecules/ μ m², a density normally found on professional APCs (35). The bilayers were subsequently blocked with 5% casein in PBS and then incubated with 100 μ M NiSO₄ to produce Ni²⁺-chelating NTA-containing lipid bilayer as previously described (13). His₆-tagged Alexa Fluor 488 pMHC complexes were then incubated with the bilayer for 5 min to incorporate the pMHC complexes into the bilayer. Unbound pMHC was washed away with assay media (HEPES-buffered saline, HBS, containing 1 mM Ca²⁺, 2 mM Mg²⁺, and 1% human serum albumin (pH 7.2)). Flow cells were warmed to 37°C, and 2×10^6 CTL were injected in 200 μ l of assay media. The moment when the CTL were injected into the flow cells defines zero time in the time point assays. The cells were imaged on a confocal fluorescence microscope (Zeiss LSM510) or an Olympus inverted IX-70 microscope.

Total internal reflection fluorescence (TIRF) microscopy imaging of CD107a (LAMP-1)

All TIRF imaging was performed on an Olympus inverted IX-70 microscope using the 60 \times /1.45 N.A. TIRF objective from Olympus. TIRF illumination was set up and aligned according to the manufacturer's instructions as described in Varma et al. (36). Flow cells containing the lipid bilayers were prepared as described above. Alexa Fluor 586-labeled anti-CD107a Fab fragments were added to the CTL to a final concentration of 10 μ g/ml. The CTL in the presence of the Fab were injected in the flow cells and images were immediately taken. The Fab fragments were present throughout the experiment. Importantly, no specific signal from fluorescent-labeled CD107a was detected by TIRF illumination when agonist pMHC was not present or when a null pMHC was introduced into the bilayer.

Image analysis

Image processing was performed using Zeiss or MetaMorph software. To assess the stability of the peripheral adhesion ring of the IS, we used the

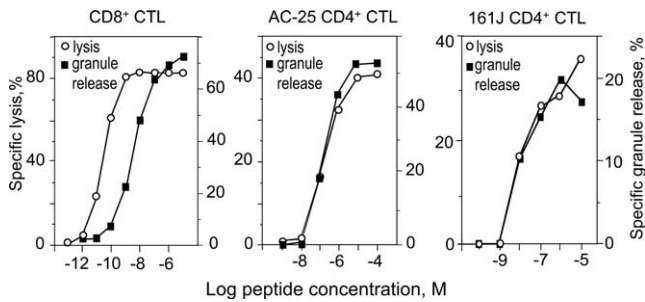


FIGURE 1. CD4⁺ CTL are less efficient lytic effectors than are CD8⁺ CTL. *Left*, Cytotoxic activity and granule release by human flu-specific CD8⁺ CTL CER43 on HLA-A2⁺ target cells (T2-DR1). *Middle*, Cytotoxic activity and granule release by human HIV Gag-specific CD4⁺ CTL AC-25 on HLA-DR1⁺ target cells (T2-DR1). *Right*, Cytotoxic activity and granule release by CD4⁺ CTL 161J vs HLA-DR4⁺ target cells (T2-DR4) sensitized with the PEVIMFSALESE (PG13) peptide from the Gag protein. The data shown are representative from three to five experiments.

linescan and journal tools in MetaMorph to generate four lines around a central point of the synapse in the first selected image of the time series for each cell. These four lines were fixed relative to the first image, and an intensity profile along each line of the ICAM-1-Cy5 fluorescence was generated for all four lines at each time point. We then evaluated the location of the pSMAC edge along each of the four lines for all images. The edge of the pSMAC was determined from the drop in the average intensity to background levels. After obtaining the location of the pSMAC edge, we subsequently calculated the change in the edge location (from time A to time B, then time B to time C, and so on) for every time point for each line. The change in the edge position along each line was then summed up and the average for the four lines was calculated and expressed in relative units (RU).

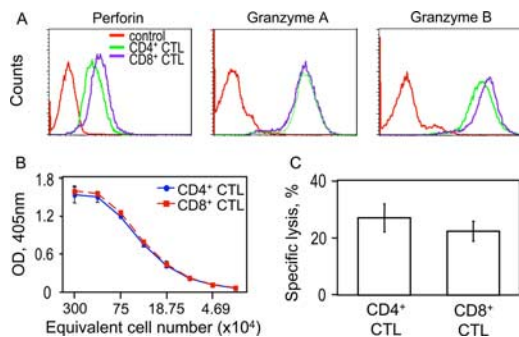


FIGURE 2. Granules isolated from CD4⁺ and CD8⁺ CTL exhibit comparable levels of serine esterase and lytic activity. *A*, Both CD8⁺ and CD4⁺ CTL express a similar level of lytic molecules. CD4⁺ AC-25, CD8⁺ CER43, and freshly isolated human CD4⁺ T cells (negative control) were stained intracellularly for either perforin or granzyme A or granzyme B and the level of expression of these lytic molecules was analyzed by flow cytometry. *B*, CD8⁺ and CD4⁺ CTL contain equal amounts of granule contents. Granule extracts from CD8⁺ and CD4⁺ CTL were adjusted for cell number so that the number of cells from which the granules were isolated per microliter of the extract was equal. The extracts were then serially diluted and tested for serine protease activity using the BLT (*N*-benzyloxycarboxyl-L-lysine thiobenzyl ester) substrate and results were read at OD 405 nm. *C*, Granules isolated from CD8⁺ and CD4⁺ CTL are equally potent in lysing target cells that do not display peptide Ags. Granule extracts from either CD4⁺ or CD8⁺ CTL were tested for the ability to lyse ⁵¹Cr-labeled T2-DR1 target cells. The assay was performed in HBSS containing 2 mM CaCl₂ for 4 h at 37°C in CO₂ incubator. The target cells were incubated with the granules, and after 4 h the culture supernatants were assayed for specific release of ⁵¹Cr. The data shown in *B* and *C* are representative of three independent assays, in which the granules from separate preparations were tested.

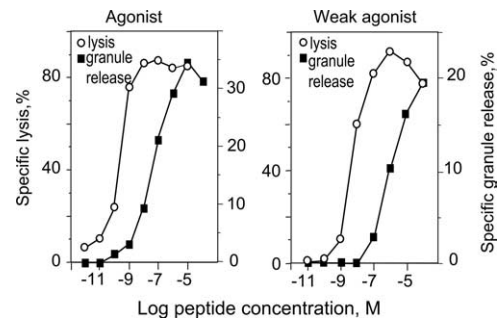


FIGURE 3. CD8⁺ CTL are still effective killers even in response to stimulation by weak agonist ligand. The human HIV-specific CD8⁺ CTL clone 68A62 recognizes the reverse transcriptase-derived agonist peptide ILKEPVHGV (IV9). A weak agonist peptide that reduces the sensitivity of the cytolytic response was derived by replacement of the IV9 glutamic acid residue at position 4 with alanine. Cytotoxic activity and granule release by 68A62 against target cells loaded with either agonist (IV9) peptide (*left*) or weak agonist (IV9-A4) peptide (*right*) are shown. The difference in the sensitivity of the two responses (lysis and granule release) by CD8⁺ CTL is not affected by stimulation through the TCR by a weak agonist peptide.

Results

CD4⁺ CTL lyse target cells bearing virus-derived peptide epitopes less efficiently than do CD8⁺ CTL

We have compared cytolytic activity of HIV-specific CD4⁺ CTL, AC-25, and flu-specific CD8⁺ CTL, CER43, by measuring percentage specific lysis and release of cytolytic granules induced by target cells sensitized with corresponding cognate peptides at various concentrations in a 4-h assay. Fig. 1 shows that CD8⁺ CTL are capable of killing target cells at very low peptide concentrations where granule release is undetectable. At peptide concentrations >10⁻⁸ M CER43 CD8⁺ CTL release increased amounts of granules, while percentage specific target lysis at this peptide concentration already reaches its maximum. In contrast, lysis by CD4⁺ CTL is only evident at peptide concentrations where there is detectable granule release, and both responses approach their maximum at the same peptide concentration (Fig. 1). The specific lysis mediated by both CD8⁺ and CD4⁺ CTL is dependent on cytolytic granules, not Fas-FasL interactions (Ref. 14) and data not shown). The observed disparity in the sensitivity of specific lysis

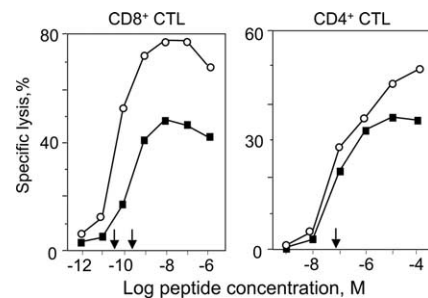


FIGURE 4. The effect on cytolytic activity by abrogating pSMAC formation with anti-LFA-1 Abs. Cytotoxic activity of CD8⁺ CTL CER43 (*left*) and CD4⁺ CTL AC-25 (*right*) against T2-DR1 target cells in the presence (+ anti-LFA-1, ■) or absence (○) of Abs against LFA-1. The concentration of cognate peptide (indicated by arrows) required to achieve half-maximal specific lysis of target cells (SD₅₀) by CD8⁺ CTL is ≈1 order of magnitude lower in the presence of LFA-1 Abs, while SD₅₀ for target cell lysis by CD4⁺ CTL is largely unaffected (the SD₅₀ value is designated by a single arrow). The data shown are representative of five independent experiments with CD8⁺ CTL CER43 and three independent experiments with CD4⁺ CTL AC-25.

Table I. *CD4⁺ CTL form very few antigen-independent ring junctions^a*

	AC-25 CD4 ⁺ CTL	CER43 CD8 ⁺ CTL
Antigen-independent ring (%)	5 ± 2	34 ± 6
Diameter of central hole in ring (μm)	3 ± 1	6 ± 3
ICAM-1 ring area (μm ²)	37 ± 16	51 ± 17

^a CTL were added to bilayers containing ICAM-1 (300 molecules/μm²) in the absence of cognate pMHC. In the absence of cognate pMHC, antigen-independent ring junctions, similar to a pSMAC, are formed by CD8⁺ CTL (13) and appear to serve as an adhesive gasket to ensure that lytic granules are released into the synaptic cleft. CD4⁺ CTL do not form these ring junctions with any significant frequency. More than 100 cells were analyzed for both CD4⁺ and CD8⁺ CTL.

of target cells by CD4⁺ and CD8⁺ CTL was not due to a difference in either quantity of cytolytic granules in CD4⁺ and CD8⁺ CTL as established by intracellular staining of lytic molecules and by measuring level of serine esterase activity or functional activity of the granules isolated from CD4⁺ and CD8⁺ CTL (Fig. 2).

The difference in peptide concentration needed to induce detectable granule release and measurable target cell lysis by CD8⁺ CTL, but not by CD4⁺ CTL, seems to be an inherent difference between CD4⁺ and CD8⁺ CTL since a separate CD4⁺ CTL clone demonstrated a similar pattern in target cell lysis and granule release as the AC-25 CD4⁺ CTL (Fig. 1 and Ref. 37). Moreover, another CD8⁺ CTL clone showed a similar dependency of granule release and target cell lysis as the CER43 CD8⁺ CTL, regardless of whether a strong or a weak agonist peptide was used to elicit CTL response (see Fig. 3). By comparing target cell lysis and granule release curves, we found that CD4⁺ CTL need to release more cytolytic granules than do CD8⁺ CTL to achieve a similar extent of specific lysis. The difference in peptide concentrations required to achieve half-maximal specific lysis and granule release provides a convenient measure of CTL effectiveness and constitutes a signature of cytolytic activity.

Table II. *Immunological synapses and horseshoe-like adhesive junctions formed by CD4⁺ and CD8⁺ CTL^a*

Analyzed Parameters	CD4 ⁺ CTL	CD8 ⁺ CTL	CD4 ⁺ CTL	CD8 ⁺ CTL
pMHC (molecules/μm ²)	500	500	25	25
IS (%)	57 ± 5	92 ± 4	55 ± 1	82 ± 6
Horseshoe-like adhesive junction (%)	22 ± 9	6 ± 5	14 ± 6	5 ± 1

^a CTL were added to bilayers containing various densities of cognate pMHC (indicated) plus ICAM-1 (300 molecules/μm²) and the percentage of cells forming synapses and horseshoe-like adhesive junctions was evaluated. All values represent means with SDs. More than 100 cells were analyzed for each condition from two to three independent experiments.

Abrogation of pSMAC formation affects the effectiveness of CD8⁺ CTL activity

The different effectiveness of target cell lysis despite equally potent granules isolated from both CD4⁺ and CD8⁺ CTL clones suggests that the AC-25 CD4⁺ CTL are less effective at targeting the released cytolytic molecules at the CTL-target cell interface. CD8⁺ CTL form Ag-independent ring junctions, perhaps to pre-establish the pSMAC that is necessary to contain released granules upon TCR triggering (13). Consistent with this, it has been shown that cytolytic granules are directed to the cSMAC (7, 8). Also, we have shown that abrogation of pSMAC formation with anti-LFA-1 Abs significantly decreased the sensitivity of target cell lysis, but not granule release, by CD8⁺ CTL (8). Based on these findings, we sought to test whether the observed difference in the effectiveness of cytolytic activity can be attributed to variations in the structure of the pSMAC formed by CD4⁺ and CD8⁺ CTL. To assess this, we measured specific target cell lysis and granule release by CD4⁺ and CD8⁺ CTL at various concentrations of cognate peptides in the presence or absence of anti-LFA-1 Abs to abrogate pSMAC formation. As expected from our previous results (8), we

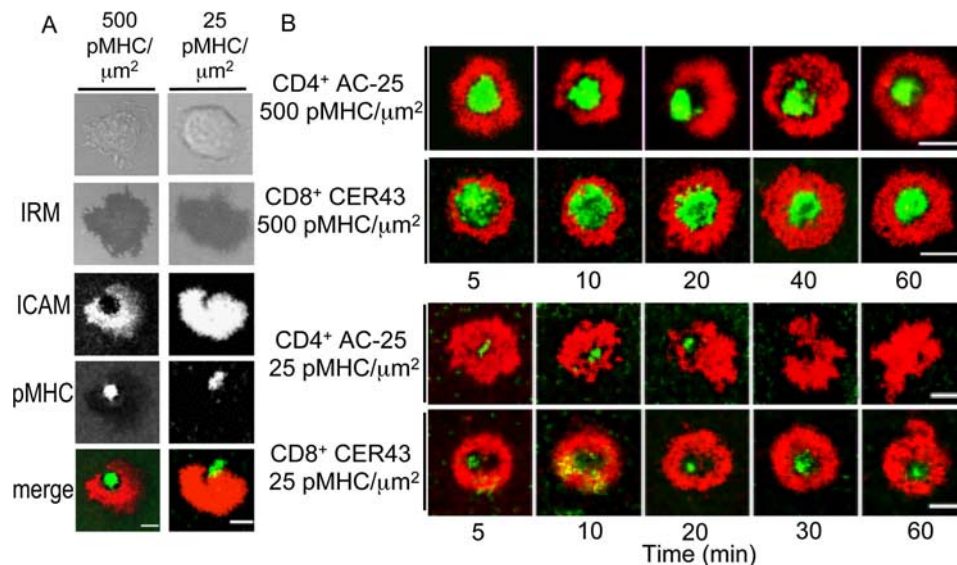


FIGURE 5. Maintenance and stability of IS formed by CD4⁺ and CD8⁺ CTL. **A**, Representative images of crescent adhesive junctions formed by CD4⁺ CTL. AC-25 CD4⁺ CTL were exposed to glass-supported bilayers containing ICAM-1 (300 molecules/μm²) and various concentrations of cognate pMHC (indicated on top). Images are taken at the level of the bilayer. IRM: Interference reflection microscopy images show the CTL contact area. Merge images: ICAM-1 is red and cognate pMHC is green. Scale bar, 5 μm. **B**, CD4⁺ and CD8⁺ CTL (indicated on the left) were exposed to glass-supported bilayers containing ICAM-1 (300 molecules/μm²) and various concentrations of cognate pMHC (indicated on the left). Images are taken at the designated times at the level of the bilayer. The average synapse duration and the percentage of cells forming and reforming synapses were determined and are presented in Table III. ICAM-1 is red and cognate pMHC is green. Scale bar, 5 μm.

Table III. Inhibition of PKC θ increases the stability of IS formed by CD4⁺ CTL^a

Analyzed Parameters	CD4 ⁺ CTL	CD8 ⁺ CTL	CD4 ⁺ CTL	CD4 ⁺ CTL + PKC θ Inhibitor	CD8 ⁺ CTL
pMHC (molecules/ μm^2)	500	500	25	25	25
Average synapse duration (min)	41 \pm 3	55 \pm 3	17 \pm 7	48 \pm 11	46 \pm 7
Stable synapses (5 min to 1 h) (%)	33 \pm 12	71 \pm 3	3 \pm 4	38 \pm 9	39 \pm 18
Form and reform 2 synapses (%)	21 \pm 7	0	16 \pm 11	8 \pm 11	11 \pm 3

^a CD4⁺ CTL were exposed to bilayers containing 300 molecules/ μm^2 ICAM-1 and cognate pMHC at indicated concentrations, and the effect of inhibiting PKC θ in CD4⁺ CTL on synapse stability was analyzed. Images were taken at 5, 10, 20, 30, 40, 50, and 60 min after the CTL were introduced to the bilayers. Based on these images, we determined the average synapse duration and the ability of CD4⁺ CTL to form mature synapses, break the synapse structure, and reform the mature synapse. The averages from two to three independent experiments are shown. At least 56 cells were analyzed for each condition. Parameters characterizing the stability of IS formed by CD8⁺ CTL at the same conditions are shown for comparison reasons.

found that the granule release response was not affected in either CD4⁺ or CD8⁺ CTL (data not shown). Strikingly, we found that the SD₅₀ for target cell lysis by CD8⁺ CTL decreased by 10-fold when anti-LFA-1 Abs were present, while abrogation of pSMAC formation in CD4⁺ CTL did not significantly affect the SD₅₀ of target cell lysis (Fig. 4). The presence of anti-LFA-1 decreased maximal specific lysis by both CD8⁺ and CD4⁺ CTL, but the effect was more pronounced for CD8⁺ CTL (Fig. 4). This demonstrates that pSMAC formation contributes to the difference in the effectiveness of cytolytic activity by CD8⁺ and CD4⁺ CTL.

AC-25 CD4⁺ CTL form fewer Ag-independent ring junctions than do CD8⁺ CTL

To elucidate variations in the formation of the pSMAC by CD4⁺ and CD8⁺ CTL, we examined the ability of CD4⁺ CTL to form Ag-independent ring junctions utilizing glass-supported lipid bilayers containing only ICAM-1 (4). We found that CD4⁺ CTL assemble Ag-independent ring junctions >6-fold less frequently than do CD8⁺ CTL (Table I). These CTL express similar levels of LFA-1, and the percentage of cells adhering was similar (data not shown and Ref. 13). This result is in agreement with the observed disparity in the ability of CD4⁺ and CD8⁺ T cells to form doughnut-like actin clouds after LFA-1 engagement, which promotes the segregation of adhesion molecules and lowers the threshold for T cell activation (38). This suggests that qualitative differences in integrin signaling favor ring junction formation by CD8⁺ CTL, but not by CD4⁺ CTL.

Difference in maintenance of the Ag-dependent IS by CD4⁺ and CD8⁺ CTL

We then analyzed the dynamic morphology of the IS at the interface between CTL and glass-supported planar bilayers containing ICAM-1 and cognate pMHC. Most activated CD8⁺ CTL form a bull's-eye synapse structure even at low density of cognate pMHC. In contrast, CD4⁺ CTL frequently form crescent- or horseshoe-like adhesive zones (Fig. 5A and Table II) similar to what has been previously observed for T cells stimulated with antagonist pMHC or pMHC that induce anergy (39, 40). In some cases such complete symmetry breaking leads to motility and the conversion of a stable junction into a crescent junction (10, 11). The increased frequency of crescent adhesive junctions formed by CD4⁺ CTL shows that the ability to maintain the pSMAC structure is reduced in CD4⁺ CTL. Indeed, the frequency of CD4⁺ and CD8⁺ CTL able to produce and maintain a stable IS was very different, especially at lower density of cognate pMHC on the bilayers (see Table III and Fig. 5B).

To directly evaluate the stability of the pSMACs formed by CD4⁺ and CD8⁺ CTL, we imaged cells attached to the bilayer at 30-s intervals from 5 to 10 min and found that the junctions produced by CD4⁺ CTL fluctuated more than those formed by CD8⁺

CTL (Movie).⁵ We then quantified the difference in the junction dynamics by tracking changes in the position of the edge (Fig. 6). The data demonstrate that the CD4⁺ CTL have a reduced capability to maintain the continuity of the pSMAC as compared with CD8⁺ CTL.

Granules released by CD4⁺ CTL "escape" from the cSMAC when the continuity of the pSMAC is broken

To understand how the stability of the IS contributes to effective granule release and target cell lysis, we next visualized granule release at the CTL contact with the bilayer by monitoring the appearance of the secretory lysosomal membrane protein CD107a (LAMP-1) within the narrow space between the CTL and bilayer. As CTL degranulate and secretory lysosomes fuse with the plasma membrane, expression of CD107a is acquired on the cell membrane (41). We thus detected granule release at the CTL-bilayer interface in real time by utilizing TIRM microscopy and a fluorescent-labeled Fab of anti-CD107a. As expected, we found that most of the CD8⁺ CTL release granules in the secretory domain surrounded by the pSMAC (Fig. 7). Lysosomal fusion with the cell membrane is also observed in CD4⁺ CTL in the secretory domain at the pSMAC-cSMAC junction; however, the release is delayed as compared with CD8⁺ CTL (A. M. Beal, N. Anikeeva, R. Varma, T. O. Cameron, P. J. Norris, M. L. Dustin, and Y. Sykulev, unpublished). Notably, CD4⁺ CTL forming horseshoe-like adhesive junction demonstrated a unique staining pattern with CD107a

⁵ The online version of this article contains supplemental material.

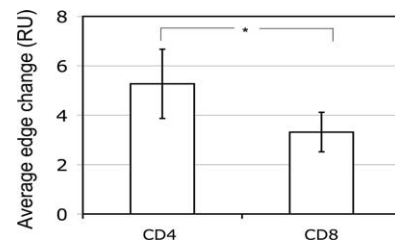


FIGURE 6. The pSMAC of the synapse formed by AC-25 CD4⁺ CTL oscillates to a greater extent. CD8⁺ and CD4⁺ CTL were added to bilayers containing ICAM-1 (300 molecules/ μm^2) and pMHC (500 molecules/ μm^2), and images were acquired from 5 to 10 min at 30-s intervals (see Movie). Modulation of the mature synapse structure was assessed as described in *Materials and Methods*. Briefly, four lines extending from a central point were drawn for each cell in the first image of the time stack. Using the intensity profile generated for each line, we determined the edge of the pSMAC at each time point. The total change in the position of the pSMAC edge was determined for each of the four lines per cell and then averaged to obtain the data for the graph. Statistical significance was assessed by the Student *t* test (*, *p* < 0.01).

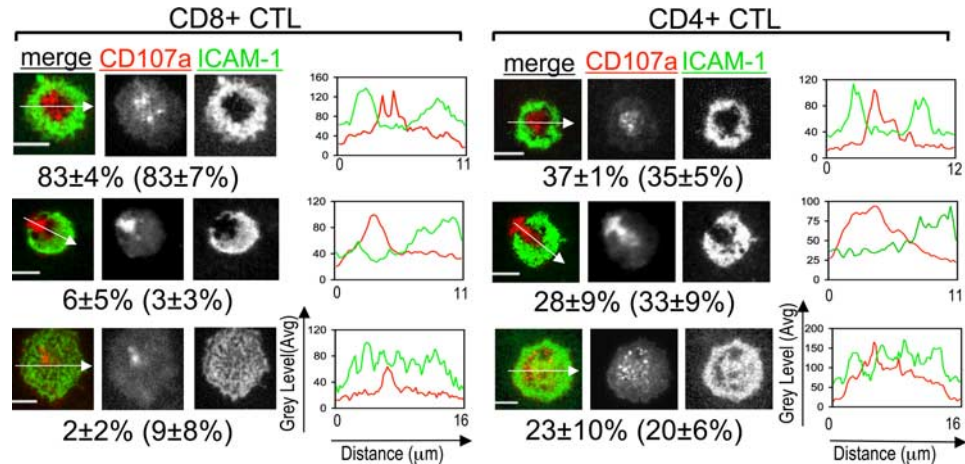


FIGURE 7. Granules released by CD4⁺ CTL are less contained within the pSMAC ring. Representative images of the patterns of CD107a accumulation observed by CD8⁺ (left) and CD4⁺ (right) CTL over 10 min after CTL exposure to bilayers. At pMHC density of 500 molecules/ μm^2 : 1) 83 \pm 4% (CD8⁺) and 37 \pm 1% (CD4⁺) of CTL show CD107a staining confined to the cSMAC; 2) 6 \pm 5% (CD8⁺) and 28 \pm 9% (CD4⁺) of CTL show CD107a staining spilling out of an unstable synapse; 3) 2 \pm 2% (CD8⁺) and 23 \pm 10% (CD4⁺) CTL show CD107a staining when a multifocal contact is formed. At pMHC density of 25 molecules/ μm^2 : 1) 83 \pm 7% (CD8⁺) and 35 \pm 5% (CD4⁺) of CTL show CD107a staining confined to the cSMAC; 2) 3 \pm 3% (CD8⁺) and 33 \pm 9% (CD4⁺) of CTL show CD107a staining spilling out of an unstable synapse; 3) 9 \pm 8% (CD8⁺) and 20 \pm 6% (CD4⁺) CTL show CD107a staining when a multifocal contact is formed. ICAM-1 is green and CD107a is red. Scale bar, 5 μm . These images are representative of three independent experiments (total number of cells analyzed was >60 cells per experimental group).

appearing to “spill out” from the cSMAC area (Fig. 7). This may be mediated by either destruction of the diffusion barrier and transport of CD107a molecules through the opening in the ring junction after release of granules into the cSMAC or due to granule release into the gap in the ring junction. Regardless, this provides evidence that in the mature synapse the pSMAC functions as a gasket containing the released molecules (granule components in particular) within the synaptic cleft.

The less stable adhesion ring of the CD4⁺ CTL IS affects lysis mediated by anti-CD3 Ab stimulation

To assess the impact of the stability of the peripheral adhesion ring on lytic activity, we measured specific lysis of ICAM-1-positive

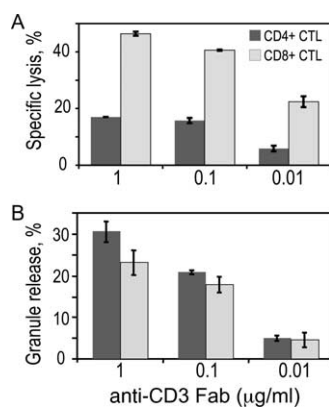


FIGURE 8. The ability to form a stable peripheral ring junctions affects target cell lysis by CTL that release granules in response to anti-CD3 stimulation. In these experiments, we assessed the ability of the CD4⁺ and CD8⁺ CTL to lyse ICAM-1-positive target cells (CIR), not expressing cognate pMHC, in response to anti-CD3 stimulation to trigger granule release as described in *Materials and Methods*. *A*, Specific lysis of CIR target cells by AC-25 CD4⁺ CTL and CER43 CD8⁺ CTL in response to anti-CD3 Fab stimulation. Anti-CD3 Fab was added at the indicated concentrations. *B*, Serine esterase release was detected in the supernatant of CTL incubated with target cells plus anti-CD3 Fab at the indicated concentrations, and the OD at 405 nm is shown. The data shown are representative from three experiments.

target cells by CD4⁺ and CD8⁺ CTL induced by soluble anti-CD3 Fab in the absence of cognate pMHC. This allowed us to unify the strength of TCR stimulation of the two clones and to exclude the difference in the contribution of CD4 and CD8 co-receptors. Both CTL clones released cytolytic granules after TCR engagement with anti-CD3 Fab, but CER43 CD8⁺ CTL, which formed a more stable pSMAC structure, demonstrated enhanced target cell lysis as compared with the AC-25 CD4⁺ CTL that formed a less stable peripheral adhesion ring (Fig. 8). This augmented lysis by the CD8⁺ CTL was not due to the release of more cytolytic granules, as the CD4⁺ CTL displayed an even greater activity of released serine esterase upon anti-CD3 Fab engagement as shown in Fig. 8. The lysis of target cells was dependent on LFA-1-ICAM-1 interactions since lysis but not granule release was inhibited by anti-LFA-1 (data not shown). These data demonstrate that the stability of the pSMAC ring junction via LFA-1-ICAM-1 interactions facilitates the sensitivity of target cell lysis by containing the released cytolytic granules to the CTL-target cell interface.

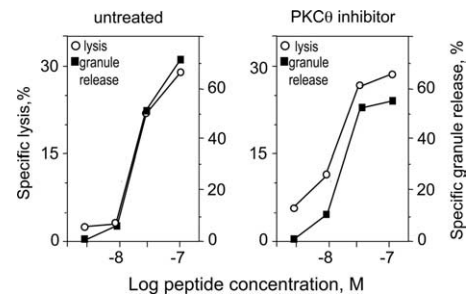


FIGURE 9. Improved sensitivity of target cell lysis by CD4⁺ CTL in the presence of a PKC θ inhibitor. Target cell lysis and granule release by AC-25 CD4⁺ CTL were analyzed at various peptide concentrations (as indicated) in the presence (right) or absence (left) of a specific inhibitor of PKC θ , and the results are depicted as percentage specific lysis and percentage granule release in the graph. This inhibitor increased the amount of stable synapses formed by CD4⁺ CTL, as shown in Table III. Inhibitor-treated CD4⁺ CTL demonstrated more effective target cell lysis, that is, increased lysis of target cells without releasing more granules. The data shown are representative of four independent experiments.

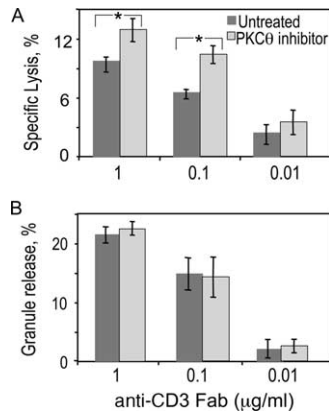


FIGURE 10. Inhibition of PKC θ also enhances lysis triggered by anti-CD3 Fab. We assessed the ability of the CD4⁺ CTL to lyse ICAM-1-positive target cells (C1R), not expressing cognate pMHC, in response to anti-CD3 stimulation to trigger granule release. *A*, Specific lysis of C1R target cells by AC-25 CD4⁺ CTL in response to anti-CD3 Fab stimulation in the presence (PKC θ inhibitor) or absence (untreated) of a PKC θ inhibitor. Anti-CD3 Fab was added at the indicated concentrations. *B*, Serine esterase release was detected in the supernatant of CTL with target cells plus anti-CD3 Fab at the indicated concentrations, and the OD at 405 nm is shown. CTL were treated as indicated in *A*. Statistical significance was assessed by the Student *t* test (*, $p \leq 0.01$).

PKC θ contributes to synapse instability and inefficient target cell lysis

We next wanted to probe the mechanism controlling pSMAC stability that was influencing the effectiveness of cytolytic activity. Recently, it has been shown that naive CD4⁺ T cells can break the symmetry of the IS structure and that this event was dependent on PKC θ (42). We thought, therefore, that PKC θ may contribute to the formation of the observed horseshoe-like adhesive junctions that do not effectively contain the released granules, resulting in ineffective target cell lysis by CD4⁺ CTL. To test directly the role of PKC θ , we utilized a selective PKC θ inhibitor, namely, Boehringer Ingelheim compound 20 (34), to inhibit PKC θ activity and to determine how this signaling molecule influences the maintenance and duration of the IS at the CD4⁺ CTL-bilayer interface. Strikingly, we found that the inhibitor increased the capability of CD4⁺ CTL to maintain a stable mature IS. In fact, in the presence of this inhibitor, the average IS duration time and the frequency of CD4⁺ CTL forming a stable IS lasting for the entire observation period became similar to those observed for CD8⁺ CTL (Table III). This increase in the stability of the IS was complemented by an enhanced effectiveness of target cell lysis, that is, an increase in the magnitude of target cell lysis without a change in granule release, when PKC θ was inhibited (Fig. 9). Granule release and the extent of specific target cell lysis by CD8⁺ CTL were very similar in the presence or absence of the inhibitor (data not shown). Furthermore, stabilization of the pSMAC by treatment with the PKC θ inhibitor enhanced the lysis mediated by CD4⁺ CTL after TCR engagement with anti-CD3 Fab, while granule release was unaffected (Fig. 10). Our results agree with findings by Grybko et al. showing that PKC θ is dispensable for granule release (43). These data demonstrate that PKC θ controls the stability of the pSMAC ring that contributes to the effectiveness of target cell lysis.

Discussion

While the formation of an adhesion ring or pSMAC in the mature IS is well appreciated, the biological significance of this event is not clearly understood. We have demonstrated herein that CD8⁺

CTL are superior in maintaining a mature, stable, and symmetrical IS, as opposed to CD4⁺ CTL, and that the mechanism regulating the maintenance of a stable peripheral adhesion ring and inducing symmetry breaking in the pSMAC requires a PKC θ -associated pathway. Furthermore, we have shown that the difference in stability of the peripheral ring junction contributes to a more effective target cell lysis by the CD8⁺ CTL. This is reflected in the “signature of cytolytic activity” of CD4⁺ and CD8⁺ CTL (Figs. 1 and 3) showing that CD4⁺ CTL need to release more cytolytic granules to achieve the same extent of target cell lysis and, therefore, appear to be less sensitive lytic effectors than CD8⁺ CTL, despite similar expression level and potency of granule contents (Fig. 2). These data indicate that not only do CTL need to release the lytic granules, but they must also confine the released lytic molecules to the CTL-target cell interface to enhance the effective delivery of the lethal hit. This is consistent with our previous findings showing that LFA-1-ICAM-1 interactions that lead to ring junction formation are not required for the release of cytolytic granules, but are essential for efficient target cell lysis by CD8⁺ CTL (8, 13). The sensitive nature of the CD8⁺ CTL response at low epitope densities is thought to be especially important for detecting and eliminating the small number of virus-infected cells during chronic viral infections.

It appears that the IS functions to regulate release and delivery of biologically active molecules by T cells. Some molecules (like lytic granule contents) need to be focused on the membrane of target cells interacting directly with CTL to ensure the destruction of virus-infected, but not uninfected cells, while other effector molecules are meant to act in a less confined fashion, for example, to regulate the activity of many other cells away from the synaptic contact (44). Whether molecules act locally or in a more distant fashion seems to be controlled by directing the pattern of their trafficking to the synaptic contact interface and subsequent release.

The stable synaptic contact that we discuss herein is that of the bull’s-eye pattern that is characteristic of the mature IS structure where adhesion molecules and TCR-pMHC segregate into pSMAC and cSMAC zones, respectively (4, 5). However, the synaptic contact between T cells and other cells of the immune system may not always lead to the formation of this stable IS structure. Indeed, immature T cells and thymocytes form stable multifocal synaptic contacts that can activate T cells (45, 46). Moreover, polarization of IFN- γ has been observed at synaptic contacts of CTL interacting with brain astrocytes that demonstrate either partial or complete segregation of adhesion molecules (47). While T cell activation and some effector functions can occur in the absence of complete molecular segregation, which is the hallmark of the mature IS (48), the latter appears to be necessary for effective delivery and focused secretion of at least some effector molecules, cytolytic granules in particular. On the other hand, it has been shown that enhancing the formation of a stable mature IS inhibits T cell proliferation and cytokine production (42, 49). More experimental data are required to determine how different changes in membrane organization at synaptic contacts affect various T cell responses at different stages of T cell activation and differentiation.

Recently published data visualizing the dynamics of IS formation by TIRF microscopy have shown that pSMAC formation and proximal signaling occur at very early time points, while the cSMAC marker molecules in microclusters can dynamically accumulate in the cSMAC zone during a much longer time frame (>30 min) after the microclusters traverse the pSMAC (36, 50). Meanwhile, in some studies the molecular markers of the cSMAC but not the pSMAC have been used to define the formation of the synapse structure, leading to the conclusion that the IS is not necessary for the efficient granule-mediated destruction of target cells

(51, 52). Since visual accumulation of the molecules in the cSMAC occurs much later than the formation of the actin ring and the pSMAC, the molecular markers of the cSMAC cannot be used to link IS formation to sensitive granule-mediated target cell lysis. In fact, it has been shown that engagement of more than five cognate pMHC complexes on target cells is sufficient to induce stable pSMAC formation and target cell death (53). Therefore, the experimental data utilizing cSMAC molecules as markers of IS formation do not discount the role of the pSMAC in concentrating the released lytic molecules. The ability of the pSMAC ring junction to concentrate lytic granules at the synaptic interface is in agreement with previous data demonstrating that only a few lytic granules are sufficient for target cell lysis (54).

To regulate effector molecule secretion, the synapse is thought to integrate several signaling platforms associated with adhesion molecules and TCR. Signaling molecules such as PKC θ , p56^{lck}, SLP76, and LAT have all demonstrated synaptic localization (5, 55, 56). Recently, it has been shown that the continuity of the pSMAC of the IS formed by naive CD4⁺ T cells is frequently broken in a mechanism that is dependent on PKC θ (42). The continuity of the pSMAC ring can be broken or maintained depending on the opposing effects of PKC θ and WASP (Wiskott-Aldrich syndrome protein), and these opposing factors regulate the balance between IS and kinapse modes in the same cell over time (42). When PKC θ was suppressed, the formation of a stable IS structure was enhanced, but this was accompanied by decreased IL-2 production (42). We propose that PKC θ may be involved in promoting formation of crescent adhesive junction that represent less efficient platforms for lysis by CD4⁺ CTL. Indeed, when PKC θ was inhibited, we observed an increased ability to maintain a stable IS by CD4⁺ CTL (see Table III). Moreover, inhibiting the activity of PKC θ in CD4⁺ CTL promoted a more efficient target cell lysis (Fig. 9). This is consistent with containment of the released lytic molecules by the pSMAC “gasket” as an essential mechanism contributing to the sensitive and efficient target cell destruction by CD8⁺ CTL (8, 13).

We acknowledge, however, that promoting a more stable synapse by inhibition of PKC θ enhanced the sensitivity of specific lysis by CD4⁺ CTL by 3-fold (0.5 log), while complete abrogation of the pSMAC by anti-LFA-1 Abs decreased the SD₅₀ for target cell lysis by CD8⁺ CTL by 10-fold (1 log), suggesting that other factors also contribute to maintaining the integrity of the pSMAC promoting more effective lysis of target cells by CD8⁺ CTL. Consistent with this, we have shown that the formation of the peripheral ring junction is increased by engagement of NKG2D receptor on CD8⁺ cytotoxic lymphocytes even in the absence of Ag (13). Moreover, it has been shown that transfection of NKG2D into CD4⁺ non-CTLs results in more stable synapses formed by these T cells (49), while in CD8⁺ T cells NKG2D expression after activation can enhance Ag-dependent IS formation and increase target cell killing (49, 57). That the abrogation of the pSMAC cannot erase the 100-fold (2-log) difference between SD₅₀ for specific target cell lysis and granule release by CD8⁺ CTL (see Figs. 1 and 4) suggests that other factors, such as the ability to kill multiple target cells (58), also contribute to the effectiveness of target cell destruction by CD8⁺ CTL.

Is the contribution of the pSMAC to the effectiveness of target cell lysis, which can vary from 3- to 10-fold, biologically significant? It has been previously shown that a 5- to 10-fold difference in cognate peptide concentration can lead to a change in the number of displayed cognate pMHC per cell by 3- to 10-fold (59). The calculation of pMHC density on target cells from the law of mass action produces similar relationships between peptide concentration and MHC occupancy with a specific peptide (60). While the

3-fold difference accounting for the sensitivity of the cytotoxicity does not seem to be crucial at high epitope density when maximum specific lysis is already achieved, the observed difference can be vital when target cells present a few cognate pMHC epitopes. For instance, Purbhoo et al. (53) have shown that one cognate pMHC complex detected at the T cell-APC interface practically does not induce target cell death, while all target cells die when as few as four specific pMHC complexes are at the interface. In another example, Ueno et al. have shown that a reduction (~2-fold) in the CTL response against target cells pulsed with low concentrations of peptide (<10⁻⁹ M) can lead to an impaired lytic activity when target cells are infected with HIV, presumably due to a low density of Ag presented by the infected target cells (61). Small changes in CTL activity observed in vitro can be translated to very serious consequences in vivo. For instance, investigation of synaptotagmin VII- (a calcium sensor) deficient mice revealed an impaired ability of KO mice to control an infection with *Listeria monocytogenes*, while the difference in the cytolytic activity mediated by CTL from these mice compared with WT controls was only ~2- to 2.5-fold less (62).

Besides enhanced adhesion mediated by a tight membrane junction at the pSMAC, this domain also appears to play a key role in directing the cytoskeleton orientation and influencing the cell polarity that are both required to exercise biological effector functions. The microtubules, which are essential for delivering the granules to the microtubule-organizing center and to the plasma membrane (12), loop through and anchor in the pSMAC (63), further demonstrating the importance of the pSMAC structure in polarizing the CTL toward the target cell. The mechanism of LFA-1 and ICAM-1 segregation to the peripheral ring junction is not clear and remains to be understood. It is thought that actin-myosin transport may be involved in the segregation process (64). Consistent with this, it has been shown that productive encounters of T cells with APCs very rapidly lead to the formation of doughnut-like actin clouds at the T cell-APC interface, and this promotes LFA-1 accumulation before TCR accumulation and lowers the threshold for subsequent T cell activation (38). Additionally, the structure of the pSMAC is more sensitive than the cSMAC to inhibition of actin polymerization, demonstrating that F-actin is required for maintaining the structure of the peripheral adhesion ring (36). In contrast, the cSMAC appears to be an active zone of exocytosis and endocytosis (see Fig. 7 and Refs. 7, 36). In fact, uptake of cytolytic molecules like granzymes by target cells is thought to involve an endocytic, perforin-dependent process (65), and we speculate that this is facilitated by an unusual membrane structure in the cSMAC zone. The cSMAC is primarily devoid of actin, talin, and some other components of the cytoskeleton that are segregated into the pSMAC area (5, 12, 36, 66, 67). This is reminiscent of mast cell degranulation, in which disruption of cortical F-actin facilitates release of inflammatory mediators (68).

A similar ring junction mediated by LFA-1-ICAM interactions is formed by other immune cells. For example, neutrophils migrating to the extravascular space penetrate through endothelial cells and form ring junctions at the neutrophil-endothelial cell interface that is likely required to initiate successful membrane fusion to allow neutrophil penetration through endothelial cells (69). The segregation of adhesion molecules at the cell-cell contact is not only a characteristic of immune cells, but also of other cells, including cells of the CNS (70). The neuronal synapse like the IS facilitates the exchange of information by directed secretion. Both synaptic structures display a functional organization of microdomains that promotes cell-cell communication through exocytosis and endocytosis at the central zone and containment of released factors within the surrounding adhesive “gasket” (71). Thus, ring

junction formation may represent a general mechanism necessary for establishing a very tight contact between two cells, which can facilitate effective delivery of biologically active molecules from one cell to another and regulate cell migration in tissues.

On the other hand, we demonstrate that the CD4⁺ CTL are still capable of killing, albeit with reduced efficiency, without forming a stable IS. This is especially evident at lower pMHC densities, a condition at which CD4⁺ CTL formed less stable synapses (Table III) and, therefore, the presence of anti-LFA-1 Abs, which disrupt the pSMAC formation, had little effect on the effectiveness of target cell killing at lower peptide concentrations (Fig. 4). The impact of anti-LFA-1 Abs became more apparent at higher peptide concentrations that give rise to higher pMHC densities promoting the formation of more stable synapses by CD4⁺ CTL (see Table III and Fig. 4). While formation of IS at CTL-target contact has been demonstrated *in vivo* (72), it will be interesting to see whether less efficient killing in context of horseshoe-like adhesive junctions can be observed in some *in vivo* settings, including chronic viral infections.

Taken together, we demonstrate that the formation of a stable adhesion ring junction, which is mediated by LFA-1-ICAM-1 interactions, is regulated in part by PKC θ . This peripheral junction serves to promote CTL selective and sensitive destruction of virally infected cells.

Acknowledgments

We thank Tasha Sims for advice on imaging and inhibition of PKC θ . We also thank Toby Starr for technical support. John Heitman and David Gutman are acknowledged for the advice regarding the CD4⁺ CTL maintenance and purification of cytolytic granules, correspondingly.

Disclosures

The authors have no financial conflicts of interest.

References

- Mentzer, S. J., B. R. Smith, J. A. Barbosa, M. A. Crimmins, S. H. Herrmann, and S. J. Burakoff. 1987. CTL adhesion and antigen recognition are discrete steps in the human CTL-target cell interaction. *J. Immunol.* 138: 1325–1330.
- Shaw, S., G. E. Luce, R. Quinones, R. E. Gress, T. A. Springer, and M. E. Sanders. 1986. Two antigen-independent adhesion pathways used by human cytotoxic T-cell clones. *Nature* 323: 262–264.
- Spitz, H., W. van Schooten, H. Keizer, G. van Seventer, M. van de Rijn, C. Terhorst, and J.-E. de Vries. 1986. Alloantigen recognition is preceded by nonspecific adhesion of cytotoxic T cells and target cells. *Science* 232: 403–405.
- Grakoui, A., S. K. Bromley, C. Sumen, M. M. Davis, A. S. Shaw, P. M. Allen, and M. L. Dustin. 1999. The immunological synapse: a molecular machine controlling T cell activation. *Science* 285: 221–227.
- Monks, C., B. Freiberg, H. Kupfer, N. Sciaky, and A. Kupfer. 1998. Three-dimensional segregation of supramolecular activation clusters in T cells. *Nature* 395: 82–86.
- Potter, T. A., K. Grebe, B. Freiberg, and A. Kupfer. 2001. Formation of supramolecular activation clusters on fresh ex vivo CD8⁺ T cells after engagement of the T cell antigen receptor and CD8 by antigen-presenting cells. *Proc. Natl. Acad. Sci. USA* 98: 12624–12629.
- Stinchcombe, J. C., G. Bossi, S. Booth, and G. M. Griffiths. 2001. The immunological synapse of CTL contains a secretory domain and membrane bridges. *Immunity* 15: 751–761.
- Anikeeva, N., K. Somersalo, T. N. Sims, V. K. Thomas, M. L. Dustin, and Y. Sykulev. 2005. Distinct role of lymphocyte function-associated antigen-1 in mediating effective cytolytic activity by cytotoxic T lymphocytes. *Proc. Natl. Acad. Sci. USA* 102: 6437–6442.
- Dobereiner, H. G., B. J. Dubin-Thaler, J. M. Hofman, H. S. Xenias, T. N. Sims, G. Giannone, M. L. Dustin, C. H. Wiggins, and M. P. Sheetz. 2006. Lateral membrane waves constitute a universal dynamic pattern of motile cells. *Phys. Rev. Lett.* 97: 038102-1–038102-4.
- Dustin, M. L. 2007. Cell adhesion molecules and actin cytoskeleton at immune synapses and kinapses. *Curr. Opin. Cell Biol.* 19: 529–533.
- Dustin, M. L. 2008. T cell activation through immunological synapses and kinapses. *Immunol. Rev.* 221: 77–89.
- Stinchcombe, J. C., E. Majorovits, G. Bossi, S. Fuller, and G. M. Griffiths. 2006. Centrosome polarization delivers secretory granules to the immunological synapse. *Nature* 443: 462–465.
- Somersalo, K., N. Anikeeva, T. N. Sims, V. K. Thomas, R. K. Strong, T. Spies, T. Lebedeva, Y. Sykulev, and M. L. Dustin. 2004. Cytotoxic T lymphocytes form an antigen-independent ring junction. *J. Clin. Invest.* 113: 49–57.
- Norris, P. J., M. Sumaroka, C. Brander, H. F. Moffett, S. L. Boswell, T. Nguyen, Y. Sykulev, B. D. Walker, and E. S. Rosenberg. 2001. Multiple effector functions mediated by human immunodeficiency virus-specific CD4⁺ T-cell clones. *J. Virol.* 75: 9771–9779.
- Appay, V., J. J. Zaunders, L. Papagno, J. Sutton, A. Jaramillo, A. Waters, P. Easterbrook, P. Grey, D. Smith, A. J. McMichael, et al. 2002. Characterization of CD4⁺ CTLs ex vivo. *J. Immunol.* 168: 5954–5958.
- Heller, K. N., C. Gurer, and C. Munz. 2006. Virus-specific CD4⁺ T cells: ready for direct attack. *J. Exp. Med.* 203: 805–808.
- Adhikary, D., U. Behrends, A. Moosmann, K. Witter, G. W. Bornkamm, and J. Mautner. 2006. Control of Epstein-Barr virus infection *in vitro* by T helper cells specific for virion glycoproteins. *J. Exp. Med.* 203: 995–1006.
- Nikiforow, S., K. Bottomly, and G. Miller. 2001. CD4⁺ T-cell effectors inhibit Epstein-Barr virus-induced B-cell proliferation. *J. Virol.* 75: 3740–3752.
- Hahn, S., R. Gehri, and P. Erb. 1995. Mechanism and biological significance of CD4-mediated cytotoxicity. *Immunol. Rev.* 146: 57–79.
- Norris, P. J., H. F. Moffett, O. O. Yang, D. E. Kaufmann, M. J. Clark, M. M. Addo, and E. S. Rosenberg. 2004. Beyond help: direct effector functions of human immunodeficiency virus type 1-specific CD4⁺ T cells. *J. Virol.* 78: 8844–8851.
- Gotch, F., J. Rothbard, K. Howland, A. Townsend, and A. McMichael. 1987. Cytotoxic T lymphocytes recognize a fragment of influenza virus matrix protein in association with HLA-A2. *Nature* 326: 881–882.
- Valitutti, S., S. Muller, M. Dessing, and A. Lanzavecchia. 1996. Different responses are elicited in cytotoxic T lymphocytes by different levels of T cell receptor occupancy. *J. Exp. Med.* 183: 1917–1921.
- Storkus, W. J., J. Alexander, J. A. Payne, J. R. Dawson, and P. Cresswell. 1989. Reversal of natural killing susceptibility in target cells expressing transfected class I HLA genes. *Proc. Natl. Acad. Sci. USA* 86: 2361–2364.
- Anikeeva, N., T. Lebedeva, M. Krosgaard, S. Y. Tetin, E. Martinez-Hackert, S. A. Kalams, M. M. Davis, and Y. Sykulev. 2003a. Distinct molecular mechanisms account for the specificity of two different T-cell receptors. *Biochemistry* 42: 4709–4716.
- Anikeeva, N., T. Lebedeva, A. R. Clapp, E. R. Goldman, M. L. Dustin, H. Mattoussi, and Y. Sykulev. 2006. Quantum dot/peptide-MHC biosensors reveal strong CD8-dependent cooperation between self and viral antigens that augment the T cell response. *Proc. Natl. Acad. Sci. USA* 103: 16846–16851.
- Stern, L. J., and D. C. Wiley. 1992. The human class II MHC protein HLA-DR1 assembles as empty $\alpha\beta$ heterodimers in the absence of antigenic peptide. *Cell* 68: 465–477.
- Chicz, R. M., R. G. Urban, W. S. Lane, J. C. Gorga, L. J. Stern, D. A. Vignali, and J. L. Strominger. 1992. Predominant naturally processed peptides bound to HLA-DR1 are derived from MHC-related molecules and are heterogeneous in size. *Nature* 358: 764–768.
- Tsomides, T. J., B. D. Walker, and H. N. Eisen. 1991. An optimal viral peptide recognized by CD8⁺ T cells binds very tightly to the restricting class I major histocompatibility complex protein on intact cells but not to the purified class I protein. *Proc. Natl. Acad. Sci. USA* 88: 11276–11280.
- Sykulev, Y., M. Joo, I. Vturina, T. J. Tsomides, and H. N. Eisen. 1996. Evidence that a single peptide-MHC complex on a target cell can elicit a cytolytic T cell response. *Immunity* 4: 565–571.
- Pasternack, M. S., C. R. Verret, M. A. Liu, and H. N. Eisen. 1986. Serine esterase in cytolytic T lymphocytes. *Nature* 322: 740–743.
- Sitkovsky, M. V. 1993. Granule exocytosis assay of CTL activation. In *Cytotoxic Cells: Recognition, Effector Functions, Generation, and Methods*. M. V. Sitkovsky and P. A. Henkart, eds. Birkhäuser, Boston, pp. 482–483.
- Borregaard, N., J. M. Heiple, E. R. Simons, and R. A. Clark. 1983. Subcellular localization of the b-cytochrome component of the human neutrophil microbicidal oxidase: translocation during activation. *J. Cell Biol.* 97: 52–61.
- Davis, J. E., V. R. Sutton, K. A. Browne, and J. A. Trapani. 2003. Purification of natural killer cell cytotoxic granules for assaying target cell apoptosis. *J. Immunol. Methods* 276: 59–68.
- Cywin, C. L., G. Dahmann, A. S. Prokopowicz, III, E. R. Young, R. L. Magolda, M. G. Cardozo, D. A. Cogan, D. Disalvo, J. D. Ginn, M. A. Kashem, et al. 2007. Discovery of potent and selective PKC- θ inhibitors. *Bioorg. Med. Chem. Lett.* 17: 225–230.
- Dustin, M. L., R. Rothlein, A. K. Bhan, C. A. Dinarello, and T. A. Springer. 1986. Induction by IL 1 and interferon-gamma: tissue distribution, biochemistry, and function of a natural adherence molecule (ICAM-1). *J. Immunol.* 137: 245–254.
- Varma, R., G. Campi, T. Yokosuka, T. Saito, and M. L. Dustin. 2006. T cell receptor-proximal signals are sustained in peripheral microclusters and terminated in the central supramolecular activation cluster. *Immunity* 25: 117–127.
- Norris, P. J., H. F. Moffett, C. Brander, T. M. Allen, K. M. O'Sullivan, L. A. Cosimi, D. E. Kaufmann, B. D. Walker, and E. S. Rosenberg. 2004. Fine specificity and cross-clade reactivity of HIV type 1 Gag-specific CD4⁺ T cells. *AIDS Res. Hum. Retroviruses* 20: 315–325.
- Suzuki, J., S. Yamasaki, J. Wu, G. A. Koretzky, and T. Saito. 2007. The actin cloud induced by LFA-1-mediated outside-in signals lowers the threshold for T-cell activation. *Blood* 109: 168–175.
- Sumen, C., M. L. Dustin, and M. M. Davis. 2004. T cell receptor antagonism interferes with MHC clustering and integrin patterning during immunological synapse formation. *J. Cell Biol.* 166: 579–590.
- Heissmeyer, V., F. Macian, S. H. Im, R. Varma, S. Feske, K. Venuprasad, H. Gu, Y. C. Liu, M. L. Dustin, and A. Rao. 2004. Calcineurin imposes T cell unresponsiveness through targeted proteolysis of signaling proteins. *Nat. Immunol.* 5: 255–265.

41. Betts, M. R., J. M. Brenchley, D. A. Price, S. C. De Rosa, D. C. Douek, M. Roederer, and R. A. Koup. 2003. Sensitive and viable identification of antigen-specific CD8⁺ T cells by a flow cytometric assay for degranulation. *J. Immunol. Methods* 281: 65–78.
42. Sims, T. N., T. J. Soos, H. S. Xenias, B. Dubin-Thaler, J. M. Hofman, J. C. Waite, T. O. Cameron, V. K. Thomas, R. Varma, C. H. Wiggins, et al. 2007. Opposing effects of PKC θ and WASp on symmetry breaking and relocation of the immunological synapse. *Cell* 129: 773–785.
43. Grybko, M. J., A. T. Pores-Fernando, G. A. Wurth, and A. Zweifach. 2007. Protein kinase C activity is required for cytotoxic T cell lytic granule exocytosis, but the θ isoform does not play a preferential role. *J. Leukocyte Biol.* 81: 509–519.
44. Huse, M., B. F. Lillemeier, M. S. Kuhns, D. S. Chen, and M. M. Davis. 2006. T cells use two directionally distinct pathways for cytokine secretion. *Nat. Immunol.* 7: 247–255.
45. Brossard, C., V. Feuillet, A. Schmitt, C. Randriamampita, M. Romao, G. Raposo, and A. Trautmann. 2005. Multifocal structure of the T cell-dendritic cell synapse. *Eur. J. Immunol.* 35: 1741–1753.
46. Hailman, E., W. R. Burack, A. S. Shaw, M. L. Dustin, and P. M. Allen. 2002. Immature CD4⁺CD8⁺ thymocytes form a multifocal immunological synapse with sustained tyrosine phosphorylation. *Immunity* 16: 839–848.
47. Barcia, C., K. Wawrowsky, R. J. Barrett, C. Liu, M. G. Castro, and P. R. Lowenstein. 2008. In vivo polarization of IFN- γ at Kupfer and non-Kupfer immunological synapses during the clearance of virally infected brain cells. *J. Immunol.* 180: 1344–1352.
48. Lee, K., A. Holdorf, M. L. Dustin, A. C. Chan, P. A. Allen, and A. S. Shaw. 2002. T cell receptor signaling precedes immunological synapse formation. *Science* 295: 1539–1542.
49. Cemerski, S., J. Das, J. Locasale, P. Arnold, E. Giuriso, M. A. Markiewicz, D. Fremont, P. M. Allen, A. K. Chakraborty, and A. S. Shaw. 2007. The stimulatory potency of T cell antigens is influenced by the formation of the immunological synapse. *Immunity* 26: 345–355.
50. Yokosuka, T., K. Sakata-Sogawa, W. Kobayashi, M. Hiroshima, A. Hashimoto-Tane, M. Tokunaga, M. L. Dustin, and T. Saito. 2005. Newly generated T cell receptor microclusters initiate and sustain T cell activation by recruitment of Zap70 and SLP-76. *Nat. Immunol.* 6: 1253–1262.
51. Faroudi, M., C. Utzny, M. Salio, V. Cerundolo, M. Guiraud, S. Muller, and S. Valitutti. 2003. Lytic versus stimulatory synapse in cytotoxic T lymphocyte/target cell interaction: manifestation of a dual activation threshold. *Proc. Natl. Acad. Sci. USA* 100: 14145–14150.
52. O'Keefe, J. P., and T. F. Gajewski. 2005. Cutting edge: Cytotoxic granule polarization and cytolysis can occur without central supramolecular activation cluster formation in CD8⁺ effector T cells. *J. Immunol.* 175: 5581–5585.
53. Purbhoo, M. A., D. J. Irvine, J. B. Huppa, and M. M. Davis. 2004. T cell killing does not require the formation of a stable mature immunological synapse. *Nat. Immunol.* 5: 524–530.
54. Lyubchenko, T. A., G. A. Wurth, and A. Zweifach. 2001. Role of calcium influx in cytotoxic T lymphocyte lytic granule exocytosis during target cell killing. *Immunity* 15: 847–859.
55. Dustin, M. L., and J. A. Cooper. 2000. The immunological synapse and the actin cytoskeleton: molecular hardware for T cell signaling. *Nat. Immunol.* 1: 23–29.
56. Saito, T., and T. Yokosuka. 2006. Immunological synapse and microclusters: the site for recognition and activation of T cells. *Curr. Opin. Immunol.* 18: 305–313.
57. Markiewicz, M. A., L. N. Carayannopoulos, O. V. Naidenko, K. Matsui, W. R. Burack, E. L. Wise, D. H. Fremont, P. M. Allen, W. M. Yokoyama, M. Colonna, and A. S. Shaw. 2005. Costimulation through NKG2D enhances murine CD8⁺ CTL function: similarities and differences between NKG2D and CD28 costimulation. *J. Immunol.* 175: 2825–2833.
58. Wiedemann, A., D. Depoil, M. Faroudi, and S. Valitutti. 2006. Cytotoxic T lymphocytes kill multiple targets simultaneously via spatiotemporal uncoupling of lytic and stimulatory synapses. *Proc. Natl. Acad. Sci. USA* 103: 10985–10990.
59. Reay, P. A., K. Matsui, K. Haase, C. Wulfling, Y. H. Chien, and M. M. Davis. 2000. Determination of the relationship between T cell responsiveness and the number of MHC-peptide complexes using specific monoclonal antibodies. *J. Immunol.* 164: 5626–5634.
60. Sykulev, Y., R. J. Cohen, and H. N. Eisen. 1995. The law of mass action governs antigen-stimulated cytolytic activity of CD8⁺ cytotoxic T lymphocytes. *Proc. Natl. Acad. Sci. USA* 92: 11990–11992.
61. Ueno, T., H. Tomiyama, M. Fujiwara, S. Oka, and M. Takiguchi. 2004. Functionally impaired HIV-specific CD8 T cells show high affinity TCR-ligand interactions. *J. Immunol.* 173: 5451–5457.
62. Fowler, K. T., N. W. Andrews, and J. W. Huleatt. 2007. Expression and function of synaptotagmin VII in CTLs. *J. Immunol.* 178: 1498–1504.
63. Kuhn, J. R., and M. Poenie. 2002. Dynamic polarization of the microtubule cytoskeleton during CTL-mediated killing. *Immunity* 16: 111–121.
64. Wulfling, C., and M. M. Davis. 1998. A receptor/cytoskeletal movement triggered by costimulation during T cell activation. *Science* 282: 2266–2269.
65. Keefe, D., L. Shi, S. Feske, R. Massol, F. Navarro, T. Kirchhausen, and J. Lieberman. 2005. Perforin triggers a plasma membrane-repair response that facilitates CTL induction of apoptosis. *Immunity* 23: 249–262.
66. Combs, J., S. J. Kim, S. Tan, L. A. Ligon, E. L. Holzbaur, J. Kuhn, and M. Poenie. 2006. Recruitment of dynein to the Jurkat immunological synapse. *Proc. Natl. Acad. Sci. USA* 103: 14883–14888.
67. Rey, M., F. Sanchez-Madrid, and A. Valenzuela-Fernandez. 2007. The role of actomyosin and the microtubular network in both the immunological synapse and T cell activation. *Front. Biosci.* 12: 437–447.
68. Nishida, K., S. Yamasaki, Y. Ito, K. Kabu, K. Hattori, T. Tezuka, H. Nishizumi, D. Kitamura, R. Goitsuka, R. S. Geha, et al. 2005. Fc ϵ R1-mediated mast cell degranulation requires calcium-independent microtubule-dependent translocation of granules to the plasma membrane. *J. Cell Biol.* 170: 115–126.
69. Shaw, S. K., S. Ma, M. B. Kim, R. M. Rao, C. U. Hartman, R. M. Froio, L. Yang, T. Jones, Y. Liu, A. Nusrat, et al. 2004. Coordinated redistribution of leukocyte LFA-1 and endothelial cell ICAM-1 accompany neutrophil transmigration. *J. Exp. Med.* 200: 1571–1580.
70. Yamada, S., and W. J. Nelson. 2007. Synapses: sites of cell recognition, adhesion, and functional specification. *Annu. Rev. Biochem.* 76: 267–294.
71. Dustin, M. L., and D. R. Colman. 2002. Neural and immunological synaptic relations. *Science* 298: 785–789.
72. Mempel, T. R., M. J. Pittet, K. Khazaie, W. Weninger, R. Weissleder, H. von Boehmer, and U. H. von Andrian. 2006. Regulatory T cells reversibly suppress cytotoxic T cell function independent of effector differentiation. *Immunity* 25: 129–141.